SAE TECHNICAL PAPER SERIES

1999-01-0483

Numerical Prediction of Brake Fluid Temperature Rise During Braking and Heat Soaking

Kwangjin Lee
Delphi Automotive Systems

SAE The Engineering Society For Advancing Mobility Land Sea Air and Space®
INTERNATIONAL

International Congress and Exposition
Detroit, Michigan
March 1-4, 1999

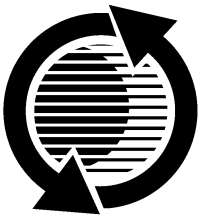

ISSN 0148-7191

Printed in USA

1999-01-0483

Numerical Prediction of Brake Fluid Temperature Rise During Braking and Heat Soaking

Kwangjin Lee
Delphi Automotive Systems

ABSTRACT

Long repetitive braking, such as one which occurs during a mountain descent, will result in a brake fluid temperature rise and may cause brake fluid vaporization. This may be a concern particularly for passenger cars equipped with aluminum calipers and with a limited air flow to the wheel brake systems. This paper describes the computer modeling techniques to predict the brake fluid temperature rise as well as other brake component temperatures during braking and heat soaking. Numerical results are compared to the measured vehicle data and the effects of relevant brake system parameters on the fluid temperature are investigated. The techniques developed in this study will help brake engineers to build a safer brake system and reduce the extensive vehicle tests currently required.

INTRODUCTION

Braking performance of a vehicle can be significantly affected by the temperature rise in the brake components. High temperature during braking may cause brake fade, premature wear, brake fluid vaporization, bearing failure, thermal cracks, and thermally-excited vibration. Therefore, it is important to predict the temperature rise of a given brake system and assess its thermal performance in the early design stage. For decades, many studies have been performed and good results have been reported in literature on the prediction of the brake disk temperature [1-7]. However, study on the brake fluid temperature is rarely found despite its importance. Recently, brake fluid vaporization has been suspected as a possible cause of some collisions and a proper inspection procedure has been recommended [8].

In this study, a typical disk brake system was modeled including the brake disk, pads, caliper, wheel, spindle, and axle in order to accurately predict the brake temperatures during a repeated braking and heat soaking. Numerical techniques were developed to consider the secondary braking factors, the division of heat at the friction interfaces, and the cooling of brake components. Numerical results were compared to the vehicle test data with a good correlation. Also investigated were the effects of the various system parameters on the fluid temperature.

BRAKE FLUID BOILING AND HEAT SOAKING

In order for the hydraulic brake system to perform its function effectively, brake fluid temperature must be kept below its boiling point. The brake fluid boiling point is significantly affected by fluid water content which is inevitable with vehicle usage. Therefore, US Department of Transport (DOT) specifies the minimum dry and wet boiling points for different grades of brake fluids in FMVSS No. 116 [9]. The majority of passenger cars in the United States operate with DOT 3 brake fluid and its boiling point is shown in Figure 1 as a function of water content [8]. DOT 3 fluid is required to have the dry boiling point of 205°C and wet boiling point of 140°C corresponding to 3.5% water absorption.

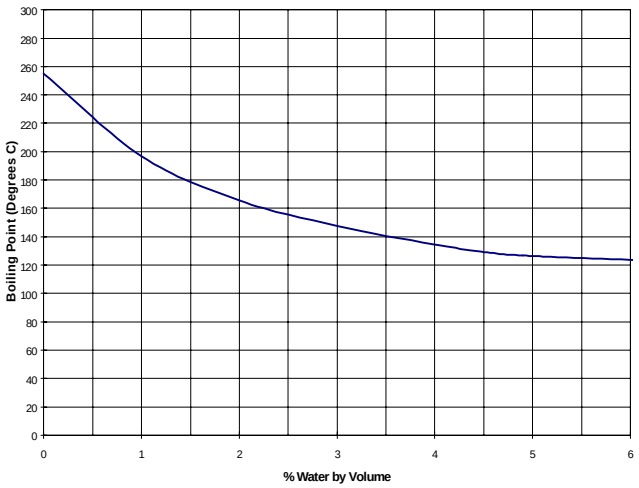

Figure 1. Boiling point vs. water content of DOT 3 brake fluid

The highest brake fluid temperature is often observed during the so-called *heat soaking* period or when the car is parked after long repetitive braking such as encountered in a high mountain descent [10]. After a vehicle is completely stopped, the hottest components, brake disks

and pads, will cool down rapidly following the Newton's law of cooling but the temperatures will continue to rise for the brake fluid and other components remote from the friction surfaces. The time for temperatures to reach peaks after the vehicle stop varies depending on the remoteness but it is in the order of 10 minutes for the brake fluid after a moderate mountain descent. Thus, heat soaking opens the possibility of brake fluid vaporization after the car has been parked for a while when an unwary driver thinks the brakes are cooled down and starts to drive.

VEHICLE ENERGY DISSIPATION DURING BRAKING

Thermal analysis of a brake system requires a frictional energy dissipation as a heat input. Frictional heat dissipation can be easily determined under the dynamometer laboratory conditions where the brake torque and the rotational speed of the brake disk are known. For vehicle braking, the frictional heat dissipation should be determined from the given vehicle and brake system parameters.

VEHICLE AND BRAKE SYSTEM CONSIDERATION – The braking forces are developed on the tire-road interface from the brake torques, τ_i, at axle i ($i = f$ for the front axle or r for the rear). The total braking force required for a vehicle with a deceleration, a_{cg}, is equal to the difference between the inertial force and the secondary braking forces such as the powertrain resistance, R_p, the tire rolling resistance, R_i, and the aerodynamic drag, D. The brake torques are generated by the wheel brake components and they can be given as a function of the line pressures, P_i,

$$\tau_f = 2 S_f \cdot P_f \tag{1}$$

$$\tau_r = 2 S_r \cdot (P_r - P_{hold}) \tag{2}$$

where S_i is the brake factor and P_{hold} is the hold-off pressure required to overcome the drum brake return spring force before any brake torque is developed.

In order to keep the rear brakes from locking before the front brakes, the proportioning valve reduces the brake line pressure at the rear brakes above the knee pressure, P_k. This behavior can be modeled as

$$P_r = (P_f - P_k) \cdot m_p + P_k \tag{3}$$

where m_p is the proportioning valve slope. The proportioning valve with two knees or with other non-linearity can be modeled with the corresponding functional relationship between P_f and P_r.

When a braking torque is applied to the tire, the tire slips on the road interface due to the tire deformation and hence the rotational speed of the tire, ω_i, is smaller than that in free rolling at the same vehicle speed. The tire slip, λ_i, during braking is defined as,

$$\lambda_i = 1 - \frac{r_i \cdot \omega_i}{V_{cg}} \tag{4}$$

where r_i is the rolling radius of the tire and V_{cg} is the vehicle speed. A simple linear relation between the tire slip and tire-road adhesion can be used as a good approximation for the mild to moderate braking on a dry road though they exhibit a highly nonlinear relation over the complete range of tire slip.

BRAKING POWER GENERATION – Using equations (1,2) and (4), the braking power dissipated, q_i, at axle i, can be given by

$$q_i = \tau_i \cdot \omega_i = \tau_i \cdot \frac{(1-\lambda_i)}{r_i} \cdot V_{cg} \tag{5}$$

The dimensionless braking power can be defined as

$$q_i^* \equiv \frac{q_i}{W \cdot V_{cg}} \tag{6}$$

where W is the vehicle weight. It can be shown that the dimensionless braking power at the front axle be derived as

$$q_f^* = \frac{(1-\lambda_f)}{\left(1 + m_p \cdot \frac{S_r}{S_f} \cdot \frac{r_f}{r_r}\right)} \left[\frac{a_{cg}}{g} - \frac{R_f}{W} - \frac{R_r}{W} - \frac{R_p}{W} - \frac{D}{W} + \frac{2 S_r \cdot P_k}{r_r \cdot W} \left(\frac{P_{hold}}{P_k} - 1 + m_p \right) \right] \tag{7}$$

where g is the acceleration due to gravity. The expressions for the rear axle can be similarly derived.

The dimensionless braking power and the tire slips are calculated for the midsize vehicle in consideration and the results at V_{cg} = 50 km/h are shown in Figure 2 as a function of deceleration rate.

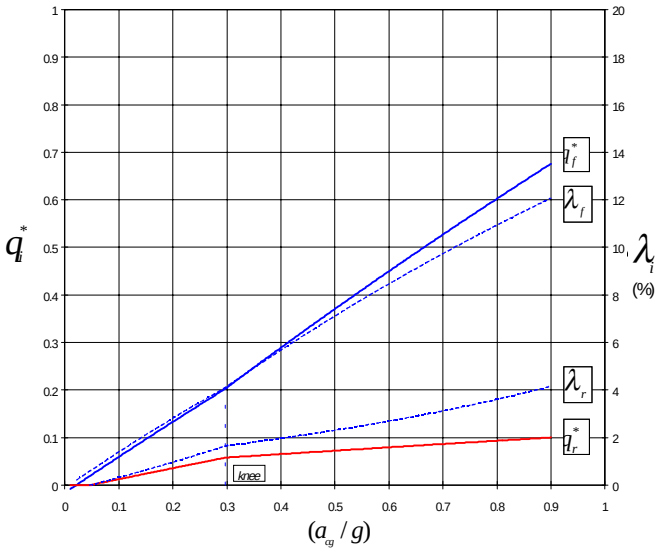

Figure 2. Brake power generation and tire slip

More fraction of braking power enters into the front brakes after the line pressure reaches the knee pressure and, as a result, the discontinuities in the slopes are observed at the knees.

EFFECTS OF THE SECONDARY BRAKING FACTORS – The secondary braking forces resist the vehicle motion and only a fraction of the total power is dissipated by the friction brake components. This fraction, ζ_b, is calculated for the midsize vehicle in consideration and the results at V_{cg} = 50 km/h are shown in Figure 3 as a function of deceleration rate.

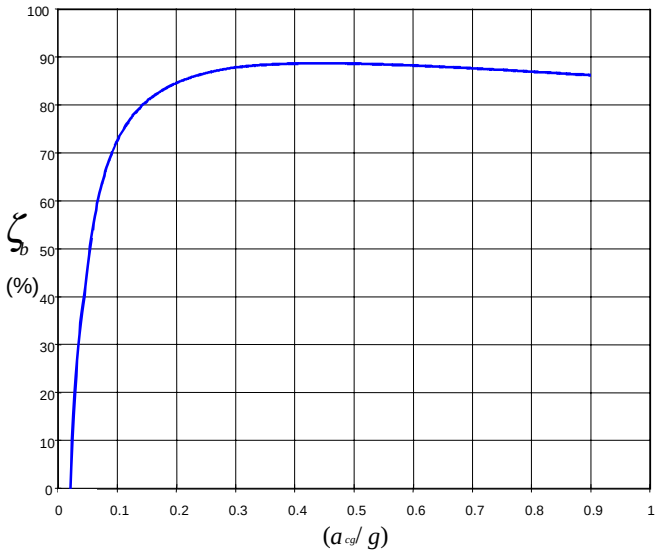

Figure 3. The fraction of power dissipated by the friction brakes

The effects of the secondary braking factors are greater at low deceleration rates and they may not be neglected even at high deceleration in order to determine the accurate amount of the frictional heat generation.

The brake balance or the distribution of the braking forces between the front and rear tires can be represented by the rear braking ratio, r_b, and the calculated results are shown in Figure 4 for the midsize vehicle in consideration at V_{cg} = 50 km/h.

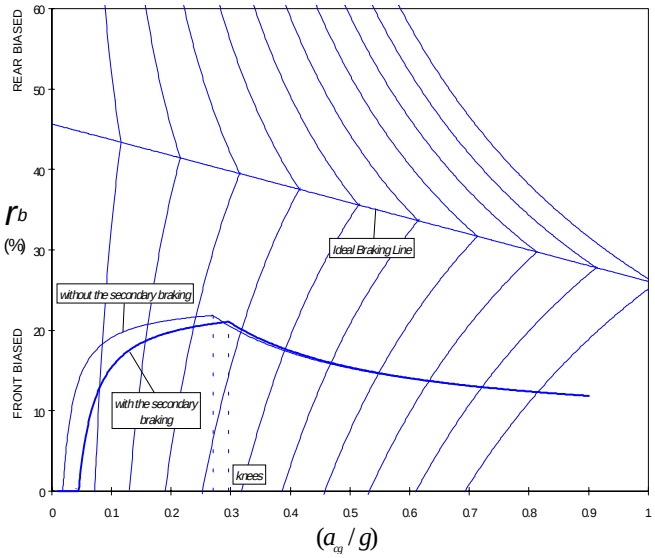

Figure 4. The effect of secondary braking on the brake balance

The calculations without including the secondary braking factors are also shown for camparison and the moderate deviation is observed at the low deceleration rates.

BRAKE THERMAL ANALYSIS

The heat dissipation at a brake corner is calculated in the previous section during a vehicle stop. In order to calculate the brake disk or pad temperatures, we need to know the fraction of the total heat into the disk or pads. The division of heat equation based on the transient solution of a semi-infinite body has been frequently used in many thermal analyses [1-4,6,7]. We will review the equation and discuss the techniques used in the paper.

DIVISION OF HEAT AT THE FRICTIONAL INTERFACE – The transient temperature, T_j, can be found in Carslaw and Jaeger [11] for the semi-infinite body, j, with the heat flux, q_j, applied at the end surface as,

$$T_j(x,t) = \frac{2q_j\sqrt{k_j \cdot t}}{K_j} \cdot ierfc\left(\frac{x}{2\sqrt{k_j \cdot t}}\right) \qquad (8)$$

where x, t, k_j, and K_j are respectively the distance from the end face, time, thermal diffusivity, and thermal conductivity of material. We use the equation (8) for two bodies (j = 1, 2) in contact at x = 0 with the frictional heat, $q_1 + q_2$, generated at the interface. Since two bodies should have equal temperature at the interface, *i.e.*,

$$T_1(0,t) = T_2(0,t) \qquad (9)$$

we have,

$$\frac{q_1}{q_1+q_2}=\frac{1}{1+\frac{K_2}{K_1}\sqrt{\frac{k_1}{k_2}}} \qquad (10)$$

Equation (10) needs to be modified to be used for a disk brake friction pair where the disk swept area is much greater than the pad contact area. Performing a similar analysis for two bodies of contact area, A_j , we have

$$\frac{q_1}{q_1+q_2}=\frac{1}{1+\frac{A_2}{A_1}\frac{K_2}{K_1}\sqrt{\frac{k_1}{k_2}}} \qquad (11)$$

CONTACT RESISTANCE FORMULATION – Though equation (11) has given satisfactory results to many thermal analyses of brakes, it may not enforce the equal temperature condition at the friction interfaces especially for a long repeated braking where the heat is transferred to remote bodies and the semi-infinite bodies no longer represent the disk brake friction pair well. The deviation in the predicted temperature depends on many factors. However, as a rule of thumb, equation (11) starts to give a moderate error for the brake system after the 10th brake application.

In this study, thermal contact resistance is used in addition to equation (11) to force the condition (9). This frictional interface model is schematically shown in Figure 5. The initial temperatures of brake disk and pad before each brake application are different since their cooling rates are different. Using thermal contact resistance at the interface, the disk and pad surface temperatures are converged to higher values in time with the rate depending on the thermal contact conductance being used for a given friction material pair.

Since reliable contact conductance data for many engineering materials are not readily available including brake friction pairs, the proper value for the thermal model was selected based on the measured temperature data. Good results were obtained with the contact conductance of 10,000-30,000 $W/m^2\ ^oC$ which agrees well to the measured conductance values of common engineering materials [12].

During cooling periods in the repeated braking process, the brake pressure is released but some amount of the drag torque remains in the wheel brake system. It is common for typical floating caliper systems with the seal retraction mechanism. This implies that there is cross-conduction between disk and pads at the interface during cooling periods and hence the cooling of disk and pads will not be completely independent. This dependency is modeled by the thermal contact conductance and the range of values, 1000-3000 $W/m^2\ ^oC$ produces good results. Also, the cross-conduction between the brake disk and pad during the heat soaking period is modeled by the thermal contact conductance of 1000 $W/m^2\ ^oC$.

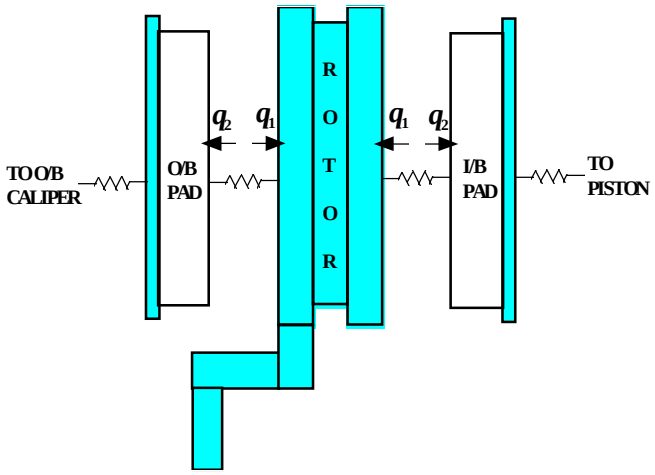

Figure 5. Heat balance at the friction interfaces

DISCRETIZATION AND NUMERICAL METHODS – The brake components are divided into small volume elements which are connected by thermal resistances to their neighboring elements. The brake disk and pads are expected to have higher thermal gradient and hence more elements were used to discretize them. Relatively smaller number of elements were used for other components such as caliper, wheel, spindle, and axle. The cyclic symmetry in the vented disk geometry was exploited and the resulting pie-shaped body was discretized. It was assumed that the heat is uniformly distributed on the disk swept area and pad contact surfaces. It should be noted that the localized contacts under some braking conditions [13,14] may result in much higher maximum temperatures on the disk and pad surfaces than are calculated under the uniform heating assumption.

Transient solutions were obtained by applying time-varying heat input, (5), during braking and zero heat input during cooling to the brake corners. Explicit formulation was used and the time step was chosen to ensure the numerical stability and convergence of the solutions. Some examples of transient solutions will be discussed later in the paper.

COOLING CONSIDERATION – The air flow around the brake components is highly complex due to the complicated body shapes and the rotating wheels in an air crossflow. Though the convection heat transfer coefficients of brake components can be measured in the wind tunnel, it is difficult to apply the results to the actual vehicle brake cooling due to the stationary ground surface and stationary wheels in typical test conditions [15]. On the other hand, progress in the computing capacity and numerical techniques has produced realistic predictions of the air flow around the brake components and the corresponding heat transfer coefficients [16,17]. Though these results can be used in the thermal analysis of the particular vehicle and brake system, the numerical process is still expensive and hence the results are not

readily available for many vehicles in production or under development. In this study, the measured cooling coefficients are used to calculate the average heat transfer coefficient, $\bar{h}$, which is defined as

$$\bar{h} = \frac{1}{A}\int h\, dA \tag{12}$$

Though the actual heat transfer coefficient will vary greatly according to the location, vehicle speed, and many other factors, the inclusion of these factors will only increase the complexity of the formulation without improving the accuracy considering the difficulty of predicting the realistic functional behavior of heat transfer coefficients. The techniques used in this study give reliable results as described in the sections below.

Heat Convection During Braking Cycles – The cooling characteristics of a heated brake system may be easily determined by measuring the cooling coefficients [17]. The brake disks are heated to the required uniform temperature and then the temperature drop is measured while the vehicle is driven at constant speeds. The temperature drop follows the Newton's law of cooling which can be written as

$$\frac{T - T_o}{T_i - T_o} = e^{-bt} \tag{13}$$

where T_i, T_o, and b are respectively the initial disk temperature, the final disk temperature, and the cooling coefficient.

The Nusselt number, Nu, generally shows a power-law relation with Reynolds number, Re,

$$Nu = C\,\mathrm{Re}^n \tag{14}$$

for both laminar and turbulent flows where the exponent, n, is commonly 0.5 for the laminar and 0.8 for the turbulent flow. Equation (14) suggests that there is a linear relation in a log-log format between the heat transfer coefficient and the vehicle speed as

$$\bar{h} = CV_{cg}^n \tag{15}$$

provided that the average air flow speed relative to the brake disk is proportional to the vehicle speed. The linear relation also exists between the cooling coefficient and the vehicle speed since the brake disk behaves as a lumped mass during cooling. Measured data reasonably support this relationship and thus only two cooling coefficients measured at two different speeds are sufficient to determine the cooling characteristics over limited ranges of two speeds selected. Corresponding heat transfer coefficients at two speeds are calculated by iterations in the computer program. The average disk heat transfer coefficient is then calculated for the given brake schedule.

Due to its rotational motion, the average heat transfer coefficient of the brake disk is greater than that of the caliper. The computations showed that the ratio between them ranges from 0.64 to 0.91 depending on brake system configurations [16]. Higher ratio was achieved when the caliper was positioned behind the axle. In this study, 0.74 was used as a proper ratio for the caliper system under consideration.

Heat Convection During Heat Soaking – During the heat soaking, the vehicle is completely stopped and the dominant mode of convection is changed to free convection from forced convection during the braking cycles. Though the brake corner is enclosed inside the wheel and tire which are in turn enclosed inside the wheel well, the formulas for the external free-convection flows were used to calculate the heat transfer coefficients of brake components since experimental or theoretical work is not available for the static brake cooling.

The radiation loss can be included during the heat soaking by considering the fourth power law of the absolute temperatures. This law can be conveniently included in the heat transfer coefficient by defining the radiant heat transfer coefficient as

$$h_r = \sigma \cdot \varepsilon \cdot \left(\hat{T} + T_\infty^2\right) \cdot \left(\hat{T} + T_\infty\right) \tag{16}$$

where σ, ε, $\hat{T}$, and T_∞ are respectively the Stefan-Boltzmann constant, the emissivity of the surface, the absolute temperatures of the disk surface and ambiance. However, due to its dependency on the surface temperature, iterations are required to calculate the accurate radiation loss.

NUMERICAL RESULTS

Transient solutions were obtained for the braking sequence in which four brake snubs are applied to the midsize car and then the vehicle is stopped for 80 seconds of cooling period. Numerical results are shown in Figure 6 as a function of time.

Temperatures are shown for various brake components. The brake fluid maintains the initial temperature implying that the heat is not transferred yet to the fluid location. Temperature fluctuation during the braking period is the highest at the friction interface and it disappears at the backplate. Note that temperatures keep increasing at the locations remote from the friction interface even after the vehicle is completely stopped at t = 80 seconds.

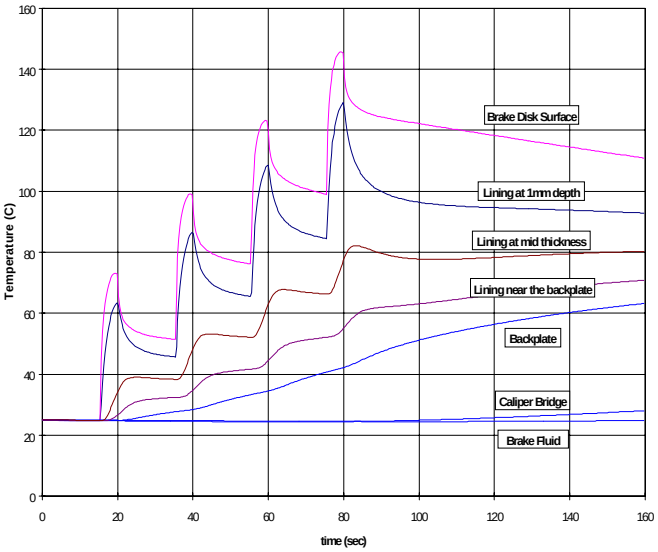

Figure 6. A transient simulation result for various brake components

GRAPHICAL USER INTERFACE – Graphical user interface was built for easier input and output data manipulation. Input parameters are grouped according to their properties such as vehicle parameters, brake system parameters, cooling information, braking schedule, geometry and material properties of components. Output nodal temperatures are presented in space and time for easier interpretation. Figure 7 shows an example of the temperature distribution in the disk brake system after a long repetitive schedule. Different ranges of temperatures are presented by the color spectrum at a specified time.

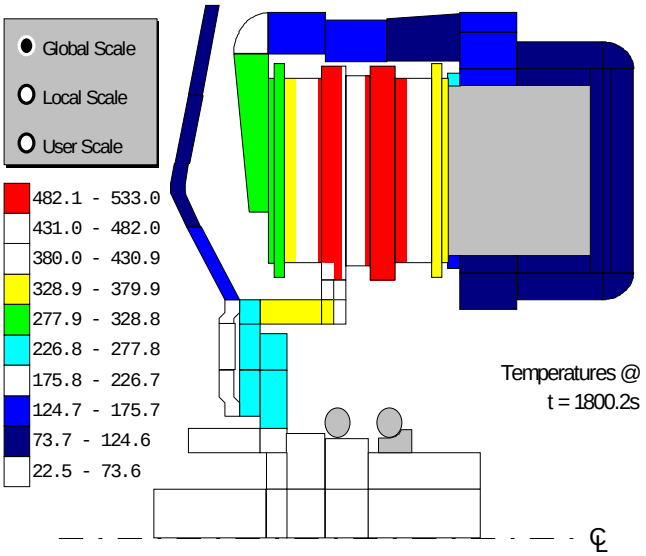

Figure 7. Graphical representation of temperature distribution in the disk brake system

Since this design tool is tailored to the automotive brake thermal analysis, it has significant advantages over commercially available computer codes.

VEHICLE TESTING AND VALIDATION

A typical midsize car was chosen for the validation of the brake thermal analysis techniques. Temperatures of the brake disk and pads were measured by embedding thermocouples at depths of 1 mm below the friction surface. A thermocouple was embedded at the center of the caliper bridge section and brake fluid temperature was measured by inserting a thermocouple in the brake fluid chamber behind the caliper piston. Brake torques and line pressures were also measured for four brake corners. The cooling coefficients were measured to be respectively 0.00281 and 0.00363 $\sec^{-1}$ at 50 and 80 km/h. The corresponding average heat transfer coefficients were respectively calculated as 34.7 and 47.0 $W/m^{2\,o}C$ at two speeds. Validation testing included 90 brake applications with a total braking period of 30 minutes. This thermal run was followed by 30 minutes of the heat soaking period. The measured temperatures are shown in Figure 8. After the vehicle is completely stopped at t = 1800 seconds, the brake disk and pads cool down rapidly following the Newton's law of cooling but the temperatures continue to rise for the brake fluid and caliper.

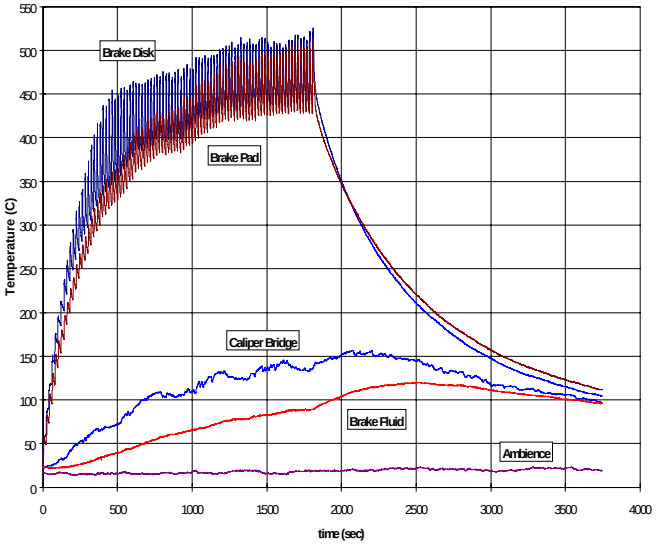

Figure 8. Measured temperatures during a repeated braking and heat soaking

This phenomenon is caused by the change of convection mode to the inefficient free convection and the high thermal gradient existed in the wheel brake system at the end of the repetitive braking.

The relevant vehicle and brake system parameters were used to calculate brake torques and pressures and good agreement was achieved with the measured averages despite the natural scatter in data. Thermal properties were measured for the semi-metallic friction material used in the brake pads and they are given in Table 1.

Table 1. Brake friction material properties

	k $m^2/s \times 10^{-6}$	K W/m^oC
semi-metallic pad	1.9	5
NAO pad	0.5	1

The transient analysis was performed and the calculated temperatures at measurement points are shown in Figure 9. All calculated temperatures at the end of the repeated braking (t = 1800 seconds) agree very well to the measured data in Figure 8. Also the calculated results represent well the cooling characteristics of the brake disk and pad, and the brake fluid temperature rise during the heat soaking period. However, the calculation predicts higher temperatures for the caliper bridge and brake fluid than measured during heat soaking. This discrepancy is in part attributed to the uncertainties in the heat transfer coefficients during the heat soaking period.

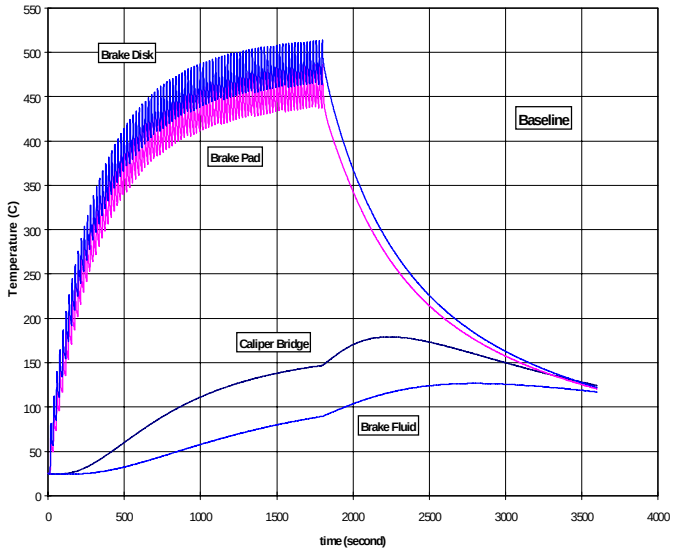

Figure 9. Calculated temperatures during a repeated braking and heat soaking

More importantly, it can be attributed to the heat conduction to the knuckle. Knuckle is modeled as a single lumped mass. Better correlation may be achieved by adding more elements to represent the knuckle.

DESIGN CASE STUDY

After the brake thermal model is validated for the tested vehicle and brake system, it can be used to conduct the parametric study to investigate the effects of design changes on the thermal performance and hence reduce the vehicle testing effort. The midsize car under consideration was used as a baseline design and various modifications were tried. Some results are discussed below.

CASE 1: BRAKE SYSTEM WITH ALUMINUM CALIPER AND SEMI-METALLIC FRICTION MATERIALS – First, we consider the case where the baseline nodular iron is replaced by the aluminum alloy for the caliper housing in order to reduce the unsprung mass. The results are shown in Figure 10 with a dashed line indicating wet fluid boiling point. At the end of brake cycles (t = 1800 seconds), the temperatures are slightly deceased for the brake disk and pad compared to those of the baseline in Figure 9 while temperatures are greatly increased for the caliper bridge and brake fluid. The caliper bridge and brake fluid have a quite high temperature difference indicating that there exists a high thermal gradient in the caliper housing during braking despite high thermal diffusivity of aluminum alloy. However, two temperatures converge quickly during the heat soaking period due to the high thermal diffusivity resulting in the higher maximum brake fluid temperature than that of the baseline vehicle.

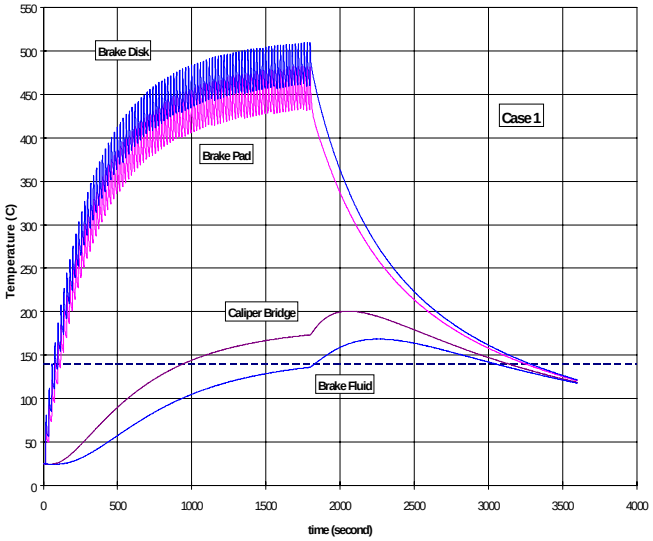

Figure 10. Calculated temperatures for the brake system with aluminum caliper and semi-metallic lining materials (Dashed line indicates wet boiling point)

CASE 2: BRAKE SYSTEM WITH ALUMINUM CALIPER AND NAO FRICTION MATERIALS – Next, in an effort to reduce the brake fluid temperature of the aluminum caliper system, the semi-metallic friction material used in the baseline vehicle was replaced by the NAO (Non-asbestos organic) friction materials. Thermal properties of NAO materials used in the calculation are given in Table 1 and the results are shown in Figure 11.

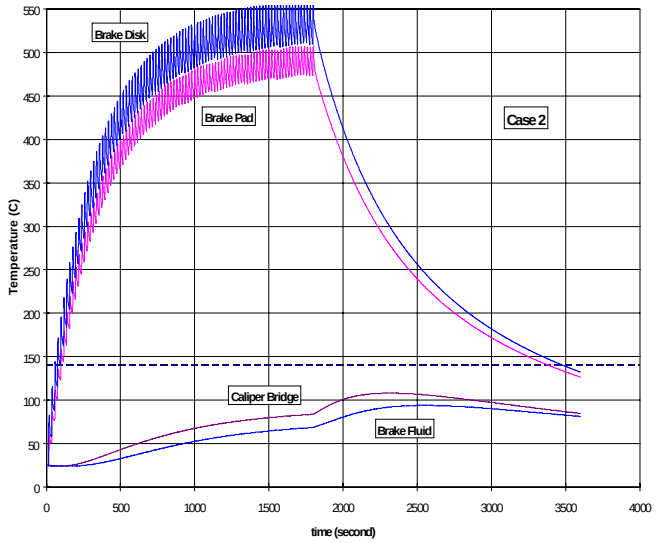

Figure 11. Calculated temperatures for the brake system with aluminum caliper and NAO lining materials (Dashed line indicates wet boiling point)

Higher thermal insulation provided by NAO materials forces more heat to the brake disk and, as a result, higher temperatures are predicted at the friction interface while lower temperature are predicted for the caliper bridge and brake fluid.

CASE 3: BRAKE SYSTEM WITH ALUMINUM CALIPER AND TWO THIRDS WORN NAO FRICTION MATERIALS – As friction materials wear out, more frictional heat transfers to the caliper resulting in higher brake fluid temperature and hence the brake system with worn friction pad should be considered. Calculations were made for the same parameters used in Case 2 except that the brake lining thickness was reduced to one thirds of full thickness in order to simulate the worn NAO friction material performance. The calculated results are shown in Figure 12.

The maximum fluid temperature is greatly increased compared to the results in Case 2 as we expected. Numerical data are given in Table 2 for the baseline and three cases considered above.

Table 2. Comparison of calculated brake fluid and disk temperatures in degrees C

	Fluid Temperature at t = 1800 sec	**Maximum Fluid Temperature during Heat Soaking**	**Maximum Brake Disk Temperature**
Baseline	89.6	126.6	513.5
Case 1	136.2	168.5	509.6
Case 2	68.7	94.0	560.7
Case 3	118.0	147.2	530.6

Though NAO material is very effective in reducing the brake fluid temperature, high fluid temperature may arise as the friction material wears out and hence the worn-out friction pad should be considered in the design process as a worst condition.

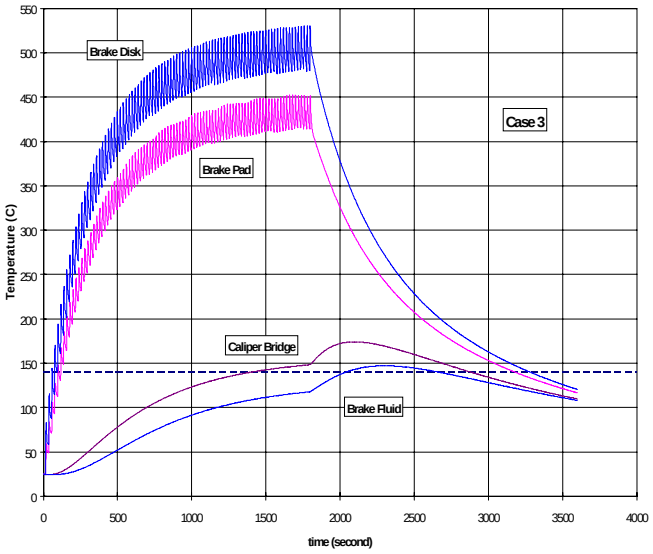

Figure 12. Calculated temperatures for the brake system with aluminum caliper and two thirds worn NAO lining materials (Dashed line indicates wet boiling point)

CONCLUSIONS

A computer model of an automotive disk brake system is developed in order to predict the temperatures of various brake components including brake disk, pads, caliper, spindle, and wheel. The frictional heat generation during the vehicle braking is determined by considering the secondary braking factors such as tire rolling resistance, powertrain resistance, aerodynamic forces, and tire slips. Cooling is considered by calculating the average convection heat transfer coefficients from the measured cooling coefficients. The vehicle testing was performed and the model was validated for the given vehicle and brake systems. The calculated results are in good agreement with the measured brake temperatures. In particular, the model predicts a realistic brake fluid temperature rise and drop during a long repeated braking and heat soaking. A parametric study was conducted to demonstrate that the brake system may have higher fluid temperature with worn-out friction materials or with more conductive friction materials.

User-friendly interface was built for brake engineers and hence the thermal analysis technique and computer model developed in this study will be very useful in the important task of predicting brake component temperatures and hence developing better brake systems.

ACKNOWLEDGMENTS

The author wishes to thank Ed Ekert, Rich Wells, and Dave Sheridan of engineering analysis for their support. The author also would like to thank co-workers involved in the vehicle testing including Joe Elliott, Alan McCready, and Bill Brown of Chassis Systems Group.

REFERENCES

1. T. P. Newcomb, “Temperatures Reached in Disc Brakes,” Journal of Mechanical Engineering Science, Vol. 2, No. 3 1960, pp. 167-177.
2. R. N. Noyes and P. T. Vickers, “Prediction of Surface Temperatures in Passenger Car Disc Brakes,” SAE 690457, 1969.
3. S. A. Abbas, N. J. Cubitt, and C. J. Hooke, “Temperature Distributions in Disc Brakes,” Proc Instn Mech Engrs, Vol. 184, Part 2A, No. 9, 1969-70, pp. 185-194.
4. R. Limpert, “The Thermal Performance of Automotive Disc Brakes,” SAE 750873, 1975.
5. A. J. Day and T. P. Newcomb, “The Dissipation of Frictional Energy from the Interface of an Annular Disc Brake,” Proc Instn Mech Engrs, Vol. 198D, No. 11, 1984, pp. 201-209.
6. D. C. Sheridan, J. A. Kutchey, and F. Samie, “Approaches to the Thermal Modeling of Disc Brakes,” SAE 880256, 1988.
7. A. Yevtushenko and E. Ivanyk, “Determination of Temperatures for Sliding Contact with Applications for Braking Systems,” Wear, Vol. 206, 1997, pp. 53-59.
8. J. E. Hunter, S. S. Cartier, D. J. Temple and R. C. Mason, “Brake Fluid Vaporization as a Contributing Factor in Motor Vehicle Collisions,” SAE 980371, 1998.
9. T. E. Ryan and T. Hinz, “Analysis of Water Content in Brake Fluid. Part I. Method Comparison: Karl Fisher Titration Versus Refractive Index,” SAE 973023, 1997.
10. K.-H. Wollenweber and R. Leiter, “Function Monitoring Brake System Temperature Monitoring Brake System,” 4th International Conference on Vehicle and Traffic Systems Technology, 1993, pp. 505-546.
11. H. S. Carslaw and J. C. Jaeger, “Conduction of Heat in Solids,” 2nd edition, Oxford Press, 1959.
12. M. Necati Ozisik, “Heat Transfer-A Basic Approach,” McGraw-Hill Book Company, 1985.
13. Kwangjin Lee and R. B. Dinwiddie, “Conditions of Frictional Contact in Disk Brakes and Their Effects on Brake Judder,” SAE 980598, 1998.
14. R. B. Dinwiddie and Kwangjin Lee, “IR-camera Methods for Automotive Brake System Studies,” in *Thermosense XX*, J. R. Snell, Jr., R. N. Wurzbach, Editors, Proceedings of SPIE, Vol. 3361, pp. 66-74, 1998.
15. G. Wickern, K. Zwicker, and M. Pfadenhauer, “Rotating Wheels-Their Impact on Wind Tunnel Test Techniques and on Vehicle Drag Results,” SAE 970133, 1997.
16. R. Krusemann and G. Schmidt, “Analysis and Optimization of Disk Brake Cooling via Computational Fluid Dynamics,” SAE 950791, 1995.
17. F. Z. Shen, D. Mukutmoni, K. Thorington, and J. Whaite, “Computational Flow Analysis of Brake Cooling,” SAE 971039, 1997.

ABOUT THE AUTHOR

Kwangjin (Mike) Lee received a B.S. and an M.S. degree in mechanical design and production engineering in 1985 and 1987 from Seoul National University. Since he received a Ph.D. degree in mechanical engineering and applied mechanics in 1993 from The University of Michigan, he has worked for Delphi Chassis Systems as a senior project engineer where his responsibility includes developing computer design software for automotive brakes and shock absorbers. His current research interests include thermoelastic problems in frictional contact, thermal analysis of brake systems, and chassis component design methodology.

Address: Technical Center Brighton MC: 483-3DB-210, 12501 E. Grand River, Brighton, MI 48116-8333, USA
Phone: 810-494-4708